IDENTIFICATION, DISTRIBUTION AND SIGNIFICANCE OF LUNAR VOLCANIC DOMES*

EUGENE I. SMITH**
Dept. of Geology, University of New Mexico, Albuquerque, N.M., U.S.A.

(Received 21 March, 1972)

Abstract. Over 300 previously unrecognized volcanic domes were identified on Lunar Orbiter photographs using the following criteria: (1) the recognition of land forms on the Moon similar in morphology to terrestrial volcanic domes, (2) structural control, (3) geomorphic discordance, and (4) the recognition of land forms modified by dome-like swellings. Many terrestrial volcanic domes are similar in morphology to lunar domes. This analogy suggests that some lunar hills are in fact extrusive volcanic domes. Many of the domes identified in this paper seem to be related to basins and craters, and with the exception of local tectonic grid control few domes are related to any observable Moon-wide pattern. Domes are not uniquely found on maria. Dome formation probably spans a wide range of lunar time and activity in areas where domes are located may be continuing to the present as revealed by the close correlation of dome distribution with the distribution of lunar transient events. The overall morphology of a lunar dome is a poor indicator of the composition of the rock that forms the dome.

1. Introduction

The form and distribution of lunar volcanic domes bear on the problem of the nature of lunar volcanism. Furthermore the distribution of domes and other probable volcanic features may provide clues to structural patterns controlling volcanism.

The Lunar Orbiter missions provided good high resolution photographs of most of the Moon and revealed over 300 previously unrecognized domes and other probable volcanic land forms. This paper discusses the criteria established for identification of lunar volcanic domes and the significance of dome distribution. Domes identified by methods presented here vary greatly in morphology from broad mare domes to irregular steep-sided cratered domes. The irregular steep-sided features are of particular interest because many resemble extrusive volcanic domes in terrestrial volcanic fields. For example, Holocene rhyolite domes in the Mono Craters in California are similar in morphology to some steep-sided lunar land forms. This analogy suggests that extrusive volcanic domes are indeed present on the Moon. Many lunar domes seem to be associated with basins and craters, and with the exception of local tectonic grid control few are related to any Moon-wide pattern.

Apollo orbital photography is now being studied to re-examine domes identified on Lunar Orbiter photographs and to survey areas where high resolution Lunar Orbiter coverage was not satisfactory. Most interpretations have not changed by viewing domes on Apollo photographs.

* Contribution No. 33 Planetary Geology Group, University of New Mexico.
** Present address: Division of Science, University of Wisconsin – Parkside, Kenosha, Wis. 53140, U.S.A.

The Moon 6 (1973) 3–31.

In this paper, I have adopted the definitions of mare material, mare and basin established by Hartmann and Wood (1971). They define *mare material* as "relatively smooth dark material... can occur in basins, craters or irregular depressions". *Mare* is defined as "a large deposit of mare material whether in a circular basin or irregular depression", and *basin* "is used to designate the largest circular depressions... Basins may or may not be flooded by mare material".

2. Definitions of Terrestrial and Lunar Domes

On Earth, the term *volcanic dome* has been broadly applied to basalt shield volcanoes, Pelean spines, tumuli and felsic extrusions. Williams (1932a), however, restricted the definition to include only "steepsided, viscous protrusions of lava forming more or less dome-shaped masses around their vents (Williams, 1932a)". Examples of volcanic domes of this type are in the Mono Craters, California (Putnam, 1932; Smith, 1970) (Figure 1). These rhyolite domes vary in diameter from less than 100 m to more than 2 km and are commonly associated with flows and craters. Flows rarely travel more than 2 km from their source. Collapse craters are shallow sags with depth-diameter (d/D) ratios varying from about 1:5 to about 1:10. Explosion craters on the other hand are deep cone-shaped craters (d/D about 1:3) up to 2 km in diameter.

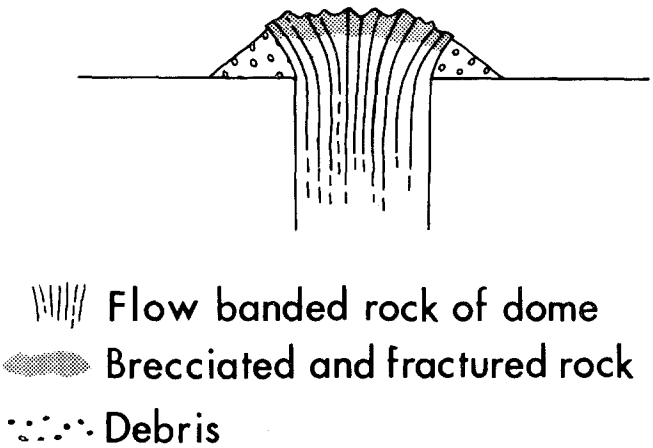

Fig. 1. Diagramatic cross section of a terrestrial volcanic dome.

In this paper, the term *lunar volcanic dome* is used in its broad sense. That is swellings on the maria, irregular swellings and steep-sided hills are referred to as domes, even though many of these features may not be true volcanic domes. Some, in fact, may be cinder cones, stratovolcanoes and shield volcanoes.

Previous lunar dome definitions are inadequate in that they only describe mare domes (Westfall, 1964). A typical mare dome is a low blister-like feature, circular to irregular in shape with diameter ranging from the limit of telescopic resolution to

about 35 km. The average mare dome diameter is about 4 km (Brungart, 196)4. Slope angle rarely exceeds 5° on the flanks of mare domes.

3. Literature Review

Previous studies of lunar domes were based primarily on telescopic observations and detailed studies of Earth-based photographs. Most of these studies described broad mare domes and various hypotheses were presented for their origin. Shaler (1903) and Spurr (1944) indicated that domes might be formed by trapping gas beneath the surface, uparching surface layers. Pickering (1903) and Baldwin (1963) showed similarities between basaltic shield volcanoes and mare domes, and Herring (1960) and Fielder (1962) advanced the idea that domes were laccolithic intrusions. Beswick (1962) suggested that domes may develop into craters. Domes mapped by the U. S. Geological Survey, Branch of Astrogeology, were interpreted as laccoliths, shield volcanoes and extrusive domes.

Arthur (1962) and Baldwin (1963) stated that domes are on the maria and noticeable clustered on both sides of the lunar equator, and Brungart (1964) substantiated this observation. Bülow (1964) indicated that domes probably existed on the lunar highlands, but could not be seen from Earth. Lunar domes were catalogued by Moore and Cattermole (1957), Abbey and Both (1958), Brungart (1964), Rae (1963, 1966) and Jamieson and Rae (1965).

Features other than mare domes were interpreted as endogenic land forms on Ranger, Orbiter and Apollo photography. Kuiper *et al.* (1965) on Ranger photographs compared several domes to tumuli on basalt flows, and Elston (1967) interpreted spines with summit pits on the northeast wall of Alphonsus as extrusive morphologies. On Lunar Orbiter photographs, McCauley (1967, 1969) interpreted hills in the Marius Hills as domes and cinder cones. O' Keefe *et al.* (1967) suggested that the Flamsteed structure was the surface expression of a ring dike, with domes and flows exposed, and Smith (1969) interpreted the Rümker Hills as a dome complex and suggested analog of domes in the Mono Craters, California to some lunar cratered domes (Smith, 1970). Eggleton (1970) suggested that several features in the Rümker and Montes Riphaeus quadrangles are stratovolcanoes. Apollo Orbital photography has revealed several probable domes (El Baz and Wilshire, 1969; El Baz, 1971; Scott *et al.*, 1971).

4. Criteria for Identification of Lunar Volcanic Domes

A. INTRODUCTION

Domes on Lunar Orbiter photographs were identified by application of a set of objective criteria which are based on (1) the recognition of land forms modified by dome-like features, (2) structural control and geomorphic discordance, and (3) characteristic surface morphology and the shape and dimensions of summit pits. Features identified by these criteria are interpreted as endogenic and not as features

related to meteorite or asteroidal impact. The number of domes identified as volcanic by these criteria is probably a conservative estimate of the total number of lunar domes, because dome identification is extremely difficult in the lunar highlands where many positive topographic features occur. A summary of criteria used to identify domes is given on Table I.

TABLE I

Summary of Criteria for Identification of Lunar Volcanic Domes

A. Land forms modified by dome-like swellings
   1. Swellings on crater walls, rims and floors.
   2. Swellings on mare ridges, and associated with rilles.

B. Structural control
   1. Swellings at the intersection of mare ridges.
   2. Swellings at the intersection of rilles.
   3. Swellings at crater intersections.

C. Geomorphic discordance
   1. Land forms superimposed on regional trends.
   2. Land forms with fresh looking appearance in areas where other features are subdued.
   3. Land forms atypical of the local terrain.

D. Morphologic criteria
   1. The presence of analogous land forms on Earth and Moon.
   2. Identification of volcanic craters associated with positive topographic features by depth-diameter technique (Smith, 1971) or crater circularity (Murray and Guest, 1970).

B. LAND FORMS MODIFIED BY DOME-LIKE SWELLINGS

Deviation from typical crater morphology, that is a distinct deviation from the shape which is typical of the majority of craters of the same size and age, is considered evidence for modification by endogenic processes. Examples are oversized central peaks, large swellings on crater walls and rims, and hills on a crater floor not related to the central peak or wall slump blocks. Swellings on mare ridges probably have an endogenic origin, since mare ridges themselves are interpreted as intrusive and/or extrusive features (Strom, 1971). Strom (1971) also noted the presence of swellings and small hills on mare ridges and interpreted them as post-mare volcanic hills. Swellings associated with rilles are also interpreted as domes.

Examples of domes in craters are: (1) a crater 8.9 km in diameter north of Mare Serenitatis enclosing a cratered central dome 3.5 km in diameter (Figure 2); (2) a crater in western Oceanus Procellarum 5.6 km in diameter with a cratered dome 2.8 km in diameter (Figure 3); (3) craters in Aitken filled with bulbous domes (boytroidal fill) (Figure 4); (4) domes in large fresh craters (Tycho, Aristarchus, Copernicus). An example of a swelling on a mare ridge is in southeastern Oceanus Procellarum (Figure 5) and domes associated with rilles are in southern Oceanus Procellarum (Figure 6) and near the crater Gruithuisen.

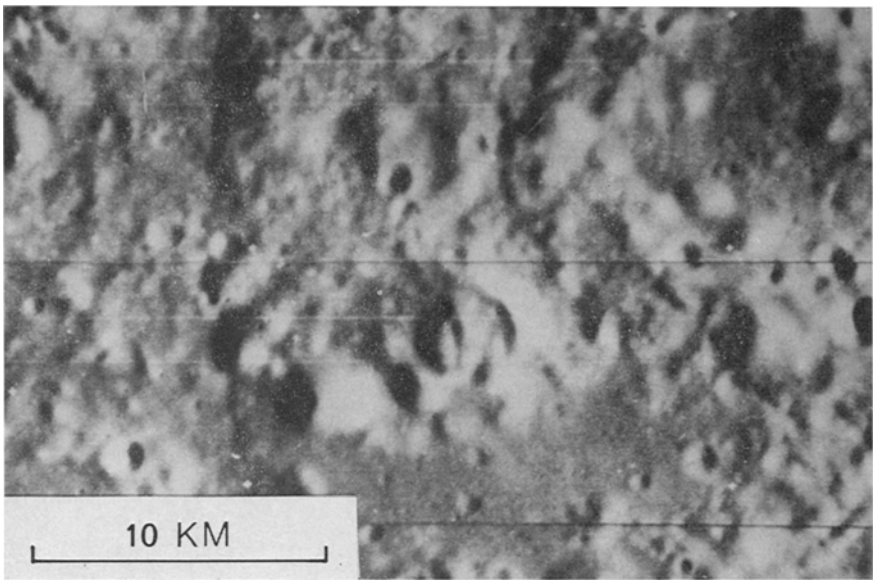

Fig. 2. A crater 8.9 km in diameter north of Mare Serenitatis which encloses a cratered dome (Lunar Orbiter 4).

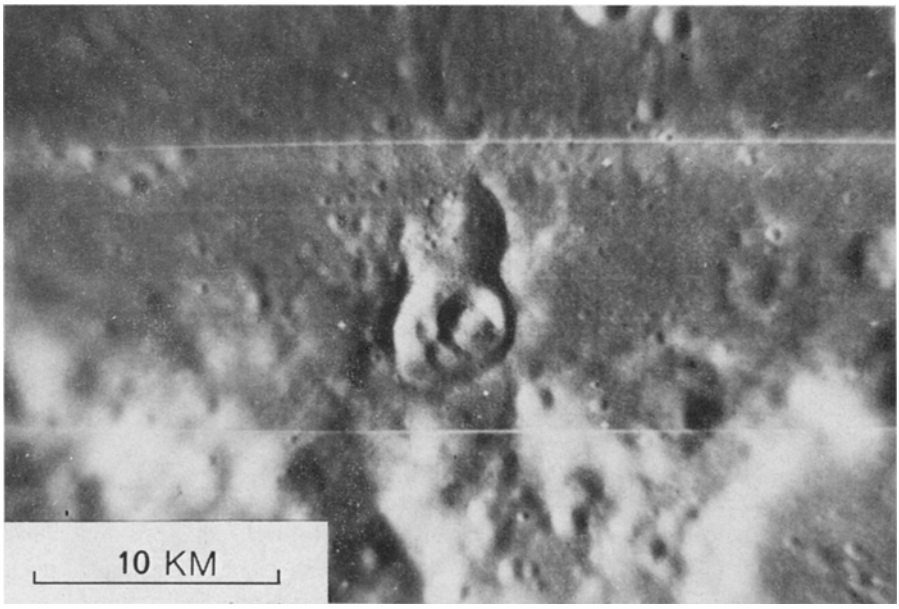

Fig. 3. A crater in western Oceanus Procellarum 5.6 km in diameter enclosing a cratered dome 2.8 km in diameter (Lunar Orbiter 4).

C. STRUCTURAL CONTROL AND GEOMORPHIC DISCORDANCE

Intersection of structural elements often controls the location of domes. For example bulbous forms at the intersection of mare ridges (Figure 7), at the intersection of rilles (Figure 8), and at the intersection of two craters (Figure 9) are interpreted as volcanic domes. Domes also may be aligned in a common direction, for example, the Hortensius domes.

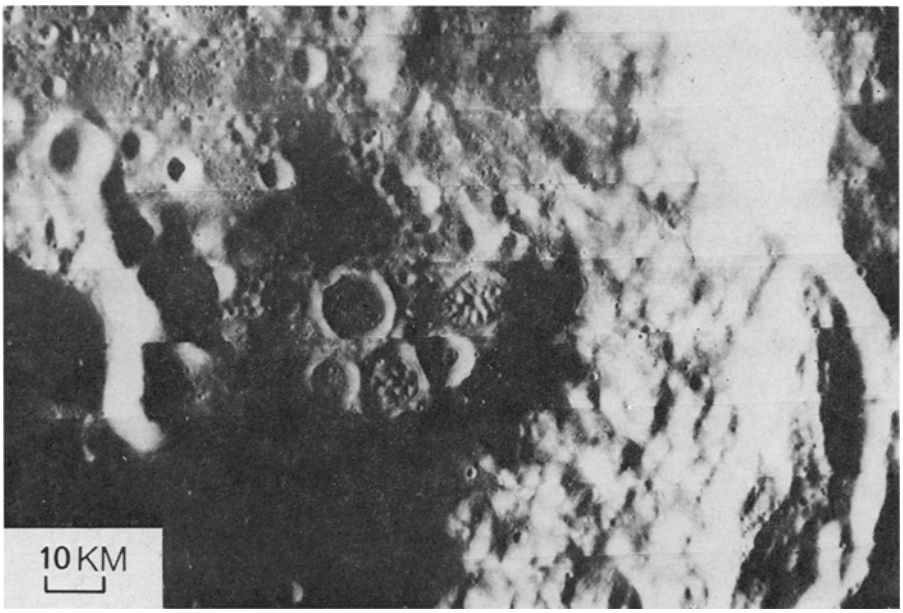

Fig. 4. Craters in Aitken filled with bulbous domes (botryoidal fill) (Lunar Orbiter 3).

Geomorphically discordant land forms are those which cut or are superimposed on regional trends, or have a sharp and fresh-looking appearance in areas where other features are subdued or those features which are atypical of the local terrain. Examples are the Gruithuisen domes (Figure 10) and a large cratered hill in an unnamed crater on the far side of the Moon (Figure 11).

D. MORPHOLOGIC CRITERIA

Information gained from study of Holocene terrestrial volcanic domes can be used as criteria for lunar dome identification. For example, Holocene rhyolite domes in the Mono Craters, California (Putnam, 1938; Smith, 1970) have characteristic surface morphologies. Their surfaces are irregular and covered with blocks; locally spines of breccia and massive rock protrude through debris (Figures 1 and 12). Flanks of the domes stand at the angle of repose (35°) and are mantled by ash, lapilli and blocks.

The overall shape of these features is due to debris resting at or near the angle of repose and not to shape or structure of the central plugs (Putnam, 1938; Smith, 1970). Similar shapes are found in domes of dacite (Williams, 1932b) and andesite (Georgalas, 1962).

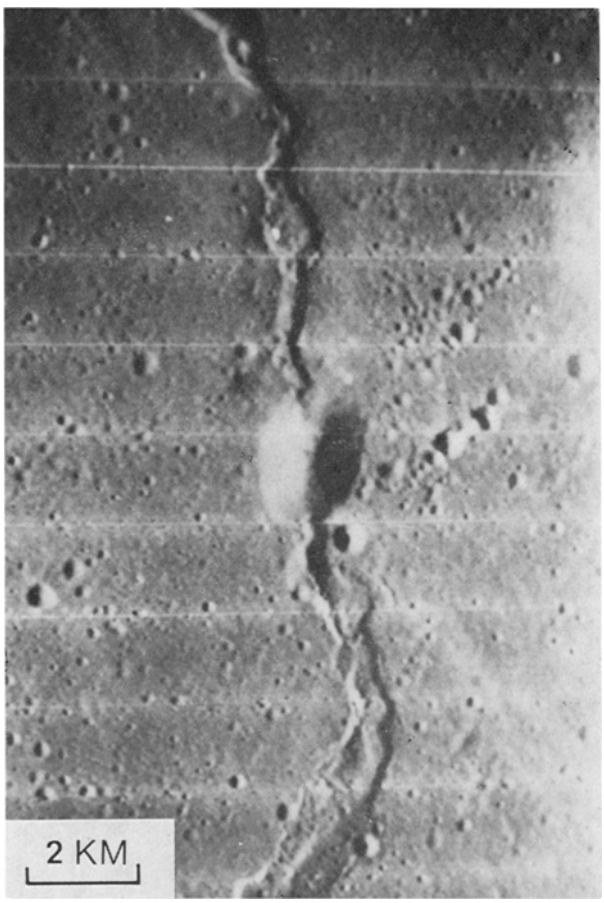

Fig. 5. A swelling on a mare ridge in southeastern Oceanus Procellarum (Lunar Orbiter 4).

Several lunar domes are covered by debris and may be analogous to domes in the Mono Craters. For example, on the floor of Copernicus there are irregular hills and cratered cones covered by blocks which are in places arranged in circular patterns (Figure 13). It is suggested that these rubble-covered hills on the floor of Copernicus are lava extrusions surrounded by debris and hence are analogous to domes in the Mono Craters.

In the Mono Craters, there is a distinct eruptive sequence (Smith, 1970) which accounts for the wide diversity of domal forms. The sequence has the following

stages (1) formation of explosion crater, (2) extrusion of a dome in the explosion crater, (3) cratering of the dome by collapse and explosions, and (4) extrusion of a dome on the floor of the crater formed in stage 3 and its subsequent cratering producing a double crater. Flows are associated with stages 2 and 4 of the sequence (Figure

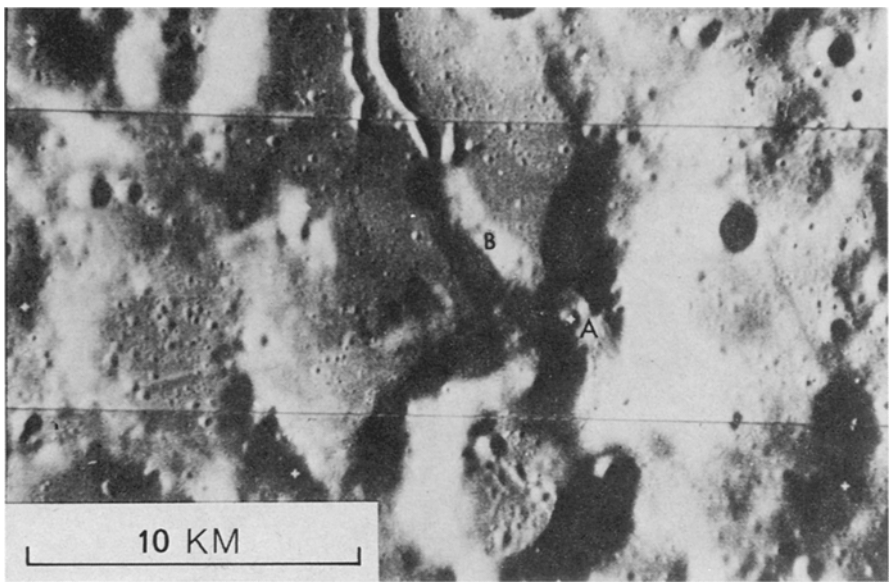

Fig. 6. A cratered dome (A) and ridge (B) associated with a rille in southern Oceanus Procellarum (Lunar Orbiter 4).

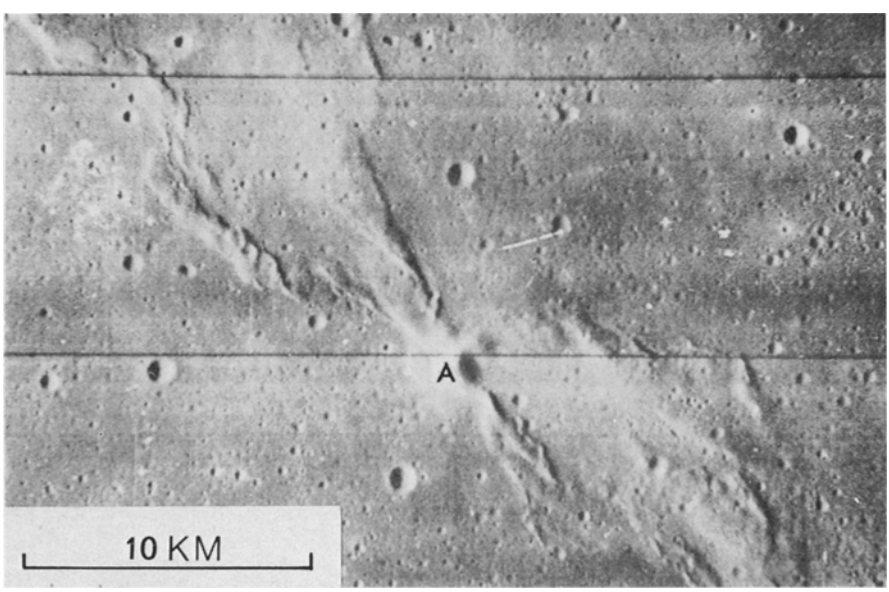

Fig. 7. A swelling (A) at the intersection of mare ridges in Oceanus Procellarum (Lunar Orbiter 4).

14). The development of a particular dome may be arrested at any stage. Parts of this sequence are well documented in dacite and andesite terrains (Smith, 1970). On the Moon, many morphologies similar to those in the Mono Craters are found associated together, for example, domes, cratered domes and double craters are observed to the west of Lacus Mortis, in Mare Frigoris and near the Alpine Valley (Figure 15).

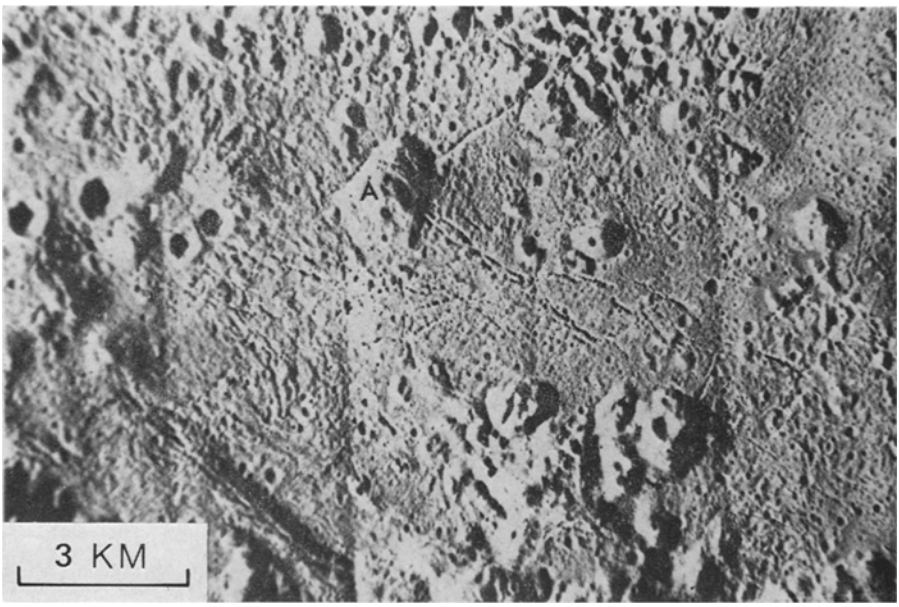

Fig. 8. Irregular hill (A) at the intersection of rilles on the floor of Copernicus (Lunar Orbiter 5).

Many lunar examples are larger than most terrestrial domes, but the difference is usually less than an order of magnitude and is not considered to be a major difficulty in making these comparisons. The fact that similar land forms exist on the Earth and Moon is evidence that some lunar domes are indeed viscous extrusive domes.

In lunar and terrestrial photographs cratered viscous extrusions may be difficult to distinguish from cratered basaltic cinder cones because the outward appearance of both features is controlled by debris on the flanks of the extrusions resting at or near the maximum angle of repose. The maximum angle of repose is dependent on particle size, shape and packing and is independent of rock composition and force of gravity. Overall shape of some volcanic hills is therefore a poor indicator of the composition of the rock composing the hill. Distinction between domes and cinder cones may be possible by the fact that they are associated with different land forms and that their crater diameter-dome diameter ratios differ. McCauley (1968) has observed similarities between cratered cinder cones and breached cones in the San Francisco volcanic field, Arizona and cones in the Marius Hills. Basaltic cinder cones in the San Francisco field may be the source of voluminous lava flows which

travel up to 20 km. Flows commonly contain well developed lava tubes and collapse depressions. On the other hand volcanic domes are associated with stubby flows which rarely flow more than 2 km and these flows are not associated with lava tubes. Domes are commonly associated with other land forms of the Mono Craters eruptive sequence (double craters, uncratered domes, dome and crater morphologies) and

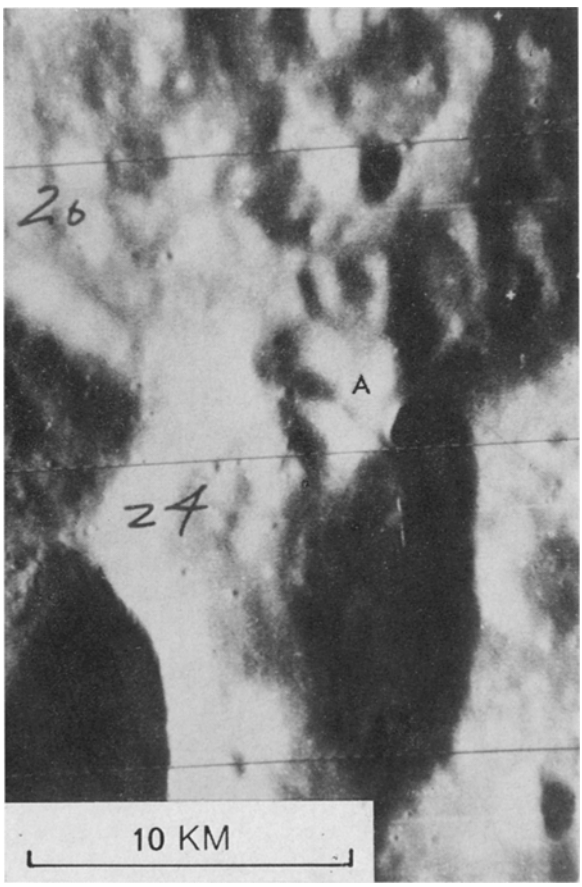

Fig. 9. Dome-like forms (A) at the intersection of two craters (Lunar Orbiter 4).

rarely with breached cones. Detailed inspection on photographs with resolution greater than 1 m will probably resolve the problem because in detail cinder cones and cratered domes differ considerably. For example, cinder cones have smooth outer slopes and bedding within the summit crater, and volcanic domes commonly have rough flanks and bedding is rare in central craters.

In photographs it may also be difficult to distinguish domes from stratovolcanoes. On the flanks of stratovolcanoes successive flow fronts and aligned craters may be

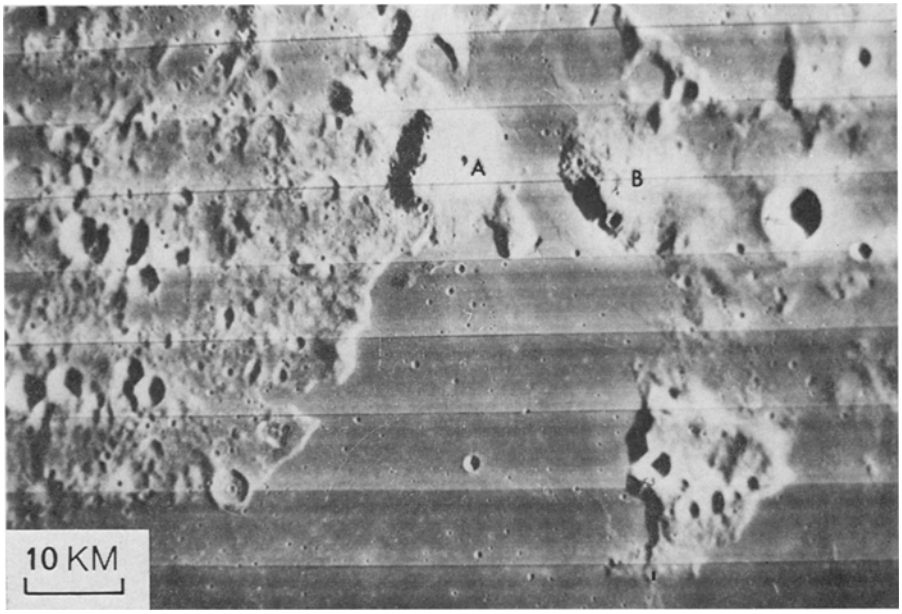

Fig. 10. The Gruithuisen domes (A and B) west of Mare Imbrium. These hills are unlike most land forms in surrounding terrain and are interpreted as volcanic domes (Lunar Orbiter 5).

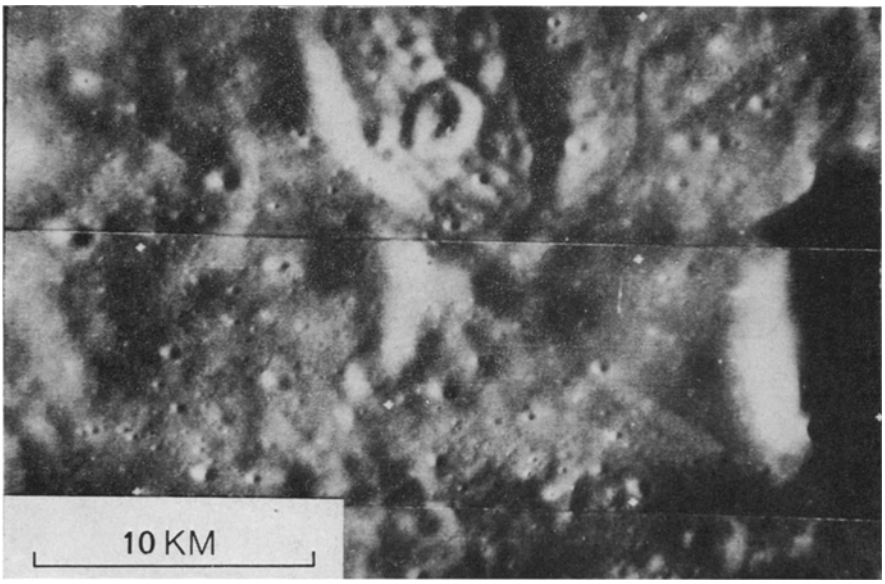

Fig. 11. A large cratered hill in an unnamed crater on the far side of the Moon. This hill is distinctly different from land forms in surrounding terrain and is interpreted as a volcanic dome (Lunar Orbiter 3).

Fig. 12. An oblique aerial photograph of Wilson Butte; a rhyolite dome in the Mono Craters, California. This dome has a shape which is typical of uncratered volcanic domes.

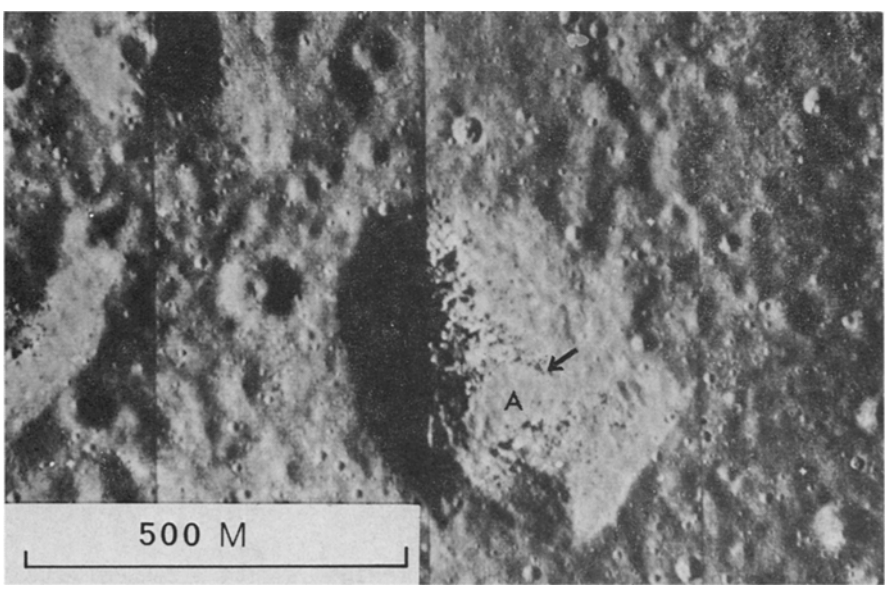

Fig. 13. An uncratered hill on the floor of Copernicus interpreted as a volcanic dome. Note ring of blocks (arrow) which may represent the margin of a circular extrusive plug (A). This plug may be surrounded by an apron of debris in the same manner as domes in the Mono Craters, California.

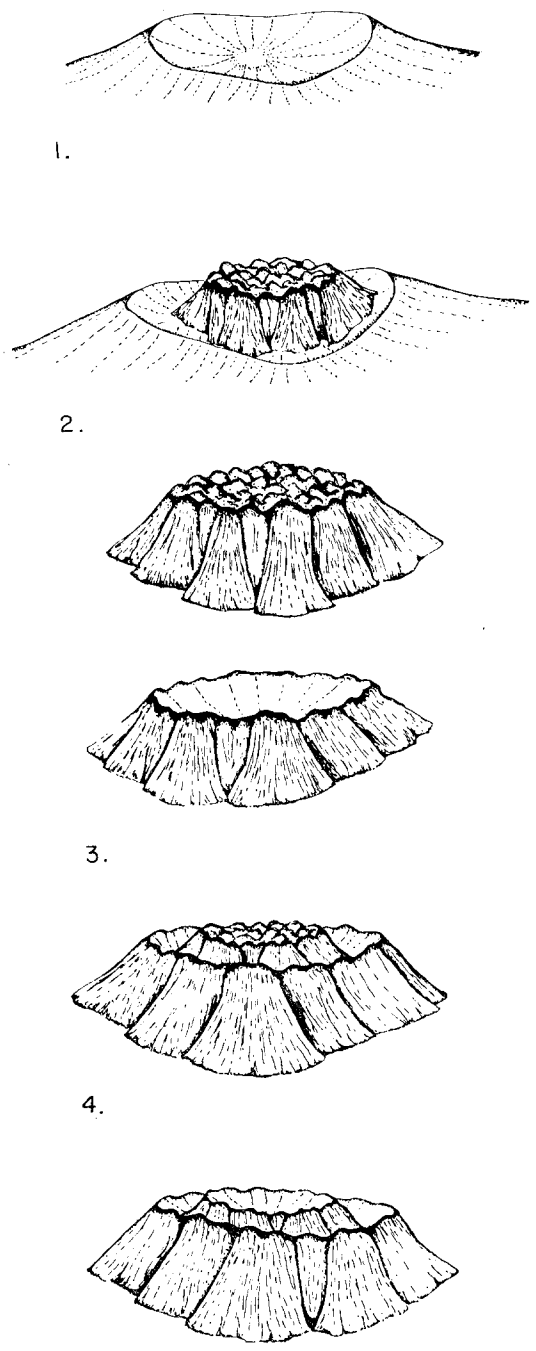

Fig. 14. The Mono Craters developmental sequence: 1. formation of an explosion crater, 2. extrusion of a dome on the explosion crater floor, 3. cratering of the dome by collapse and explosions, and 4. extrusions of a dome on the floor of the crater formed in stage 3 and its subsequent cratering producing a double crater.

present. These features are rare on the flanks of domes. An example of a possible lunar stratovolcano is in the Rümker Hills (Figure 16). Other examples are in the Rümker and Montes Riphaeus quadrangles (Eggleton, 1970).

The base-diameter/summit-crater-diameter ratio may be used as a criterion to distinguish between cratered domes, cinder cones and stratovolcanoes on photographs even though fields overlap. The ratio for five domes varies from 0.4–0.7. This compares to values of 0.17–0.5 for 35 basaltic cinder cones and 0.05–0.20 for eight strato- and shield- volcanoes. The ratio for lunar cratered hills varies from 0.2–0.9.

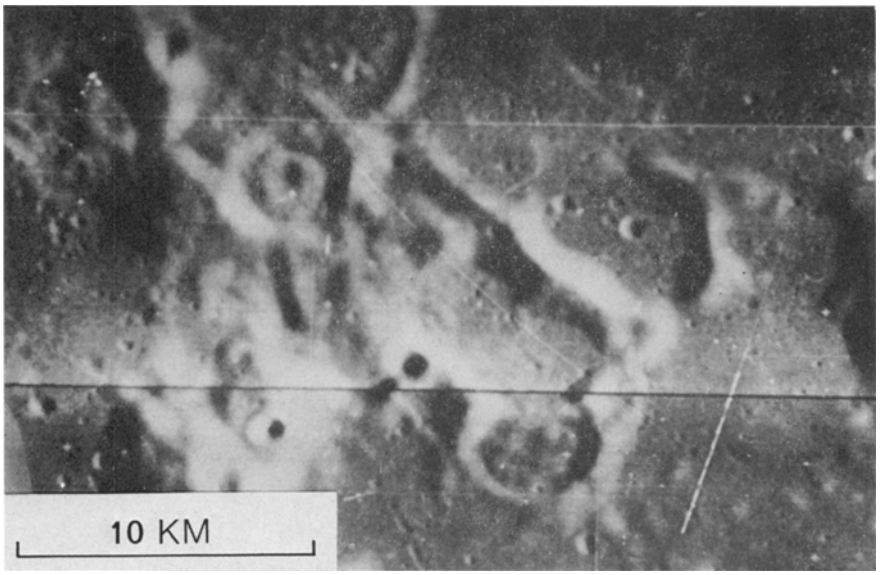

Fig. 15. Associated domes, dome in crater and cratered domes in Mare Frigoris. These features may be analogous to domes in the Mono Craters and may develop through stages similar to those of the Mono Craters developmental sequence.

Quantitative morphologic criteria include the depth-diameter ratio of craters 3.5 km in diameter (Smith, 1971). Terrestrial and lunar craters show consistent differentiation into two fields *i.e.*, a low depth/diameter field of impact craters and a high depth/diameter field of volcanic craters. If a summit crater on a lunar hill is identified as a volcanic crater, it is probable that the hill itself has a volcanic origin. The technique of Murray and Guest (1970) based on crater roundness can be used to suggest origin of large lunar craters. If a crater is interpreted as volcanic by this method, bulbous features associated with the crater may have an endogenic origin.

5. Distribution of Lunar Domes

Domes identified in this study, previously identified domes, sinuous and straight rilles and dark halo craters are plotted on Figure 17 and listed in Table II. Density

of domes and other endogenic features is plotted on Figure 18. On Table II each dome is graded A to E indicating the level of its documentation (*i.e.*, grade A indicates a well-documented dome, and E a poorly-documented dome). Land forms which are now poorly documented are an obvious choice for re-examination when high quality photography becomes available. The following conclusions are based on Figures 17 and 18.

Fig. 16. The Rümker Hills, a volcanic dome complex in the Oceanus Procellarum. A possible stratovolcano is at A. Possible lobate flow fronts associated with the stratovolcano are at B (Lunar Orbiter 4).

(1) Dome distribution is not random; domes are preferentially found (a) about the margins of basins and irregular depressions both on mare and marginal highlands materials; (b) on crater floors, walls and rims; (c) in the highlands on isolated smooth material not clearly associated with recognizable basins and in mountainous highland terrain.

(2) Domes are closely associated with sinuous rilles and dark halo craters. The

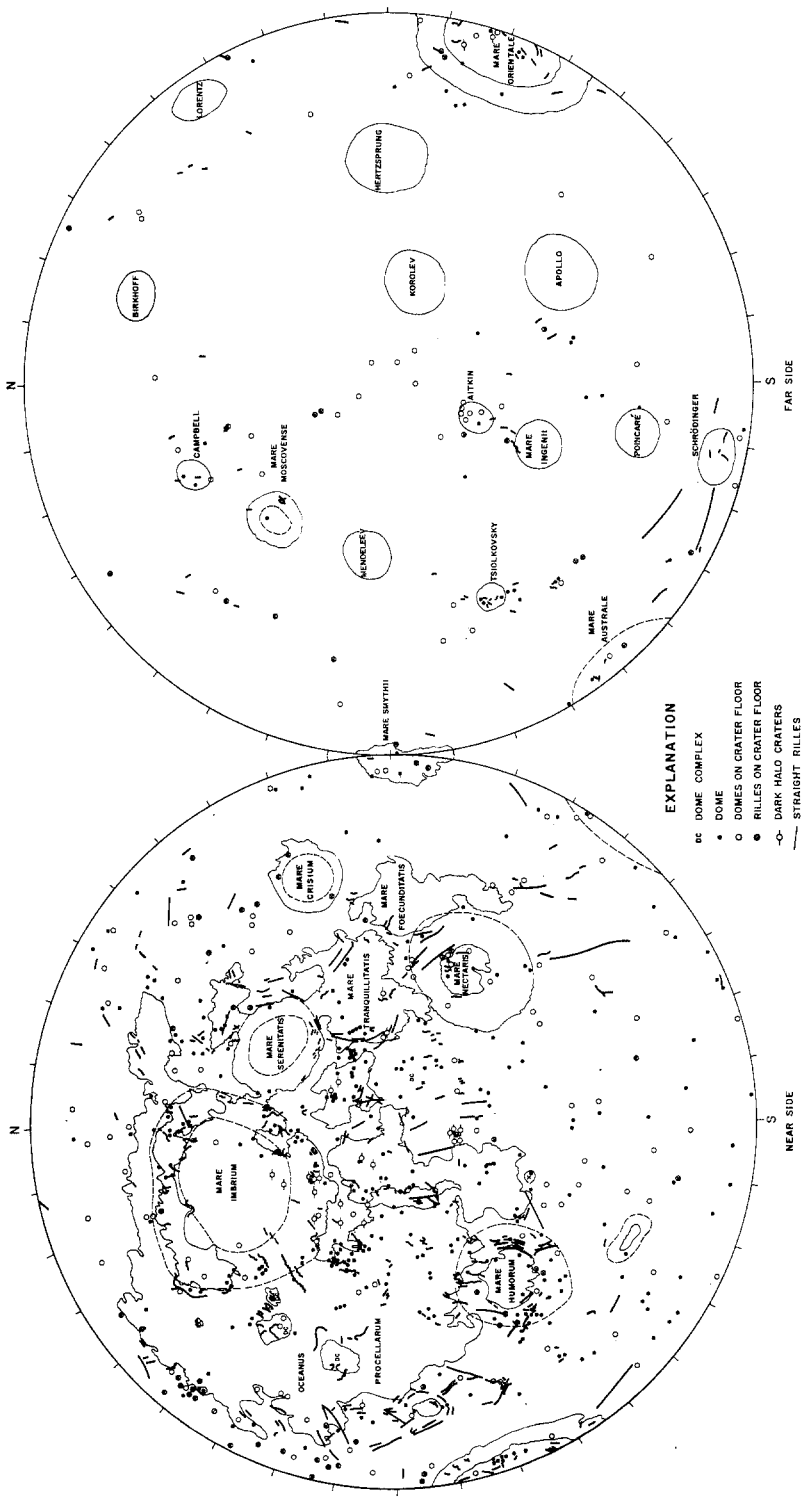

Fig. 17. Map showing the distribution of volcanic domes, sinuous and straight rilles and dark halo craters on the Moon.

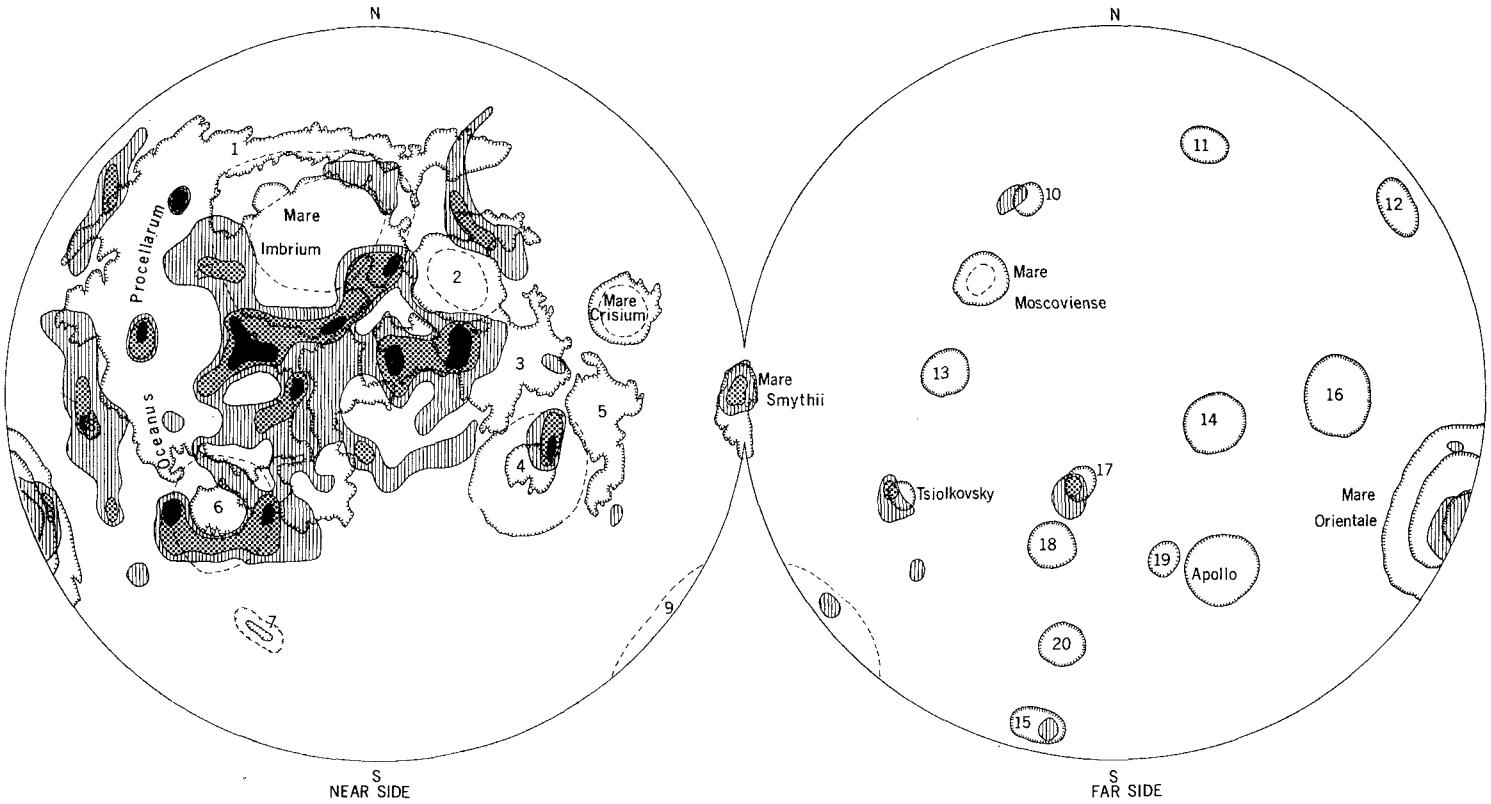

Fig. 18. Contoured distribution map of volcanic land forms on the Moon. Parallel lines indicate a density of between 3 and 5 endogenic features /40000 km^2; squares, a density between 6 and 10; and the dark pattern over 10 endogenic features/40000 km^2. Base map is a Lambert azimuthal equal-area projection. – 1. Mare Frigoris, 2. Mare Serenitatis, 3. Mare Tranquilitatis, 4. Mare Nectaris, 5. Mare Foecunditatis, 6. Mare Humorum, 7. Schiller, 8. Grimaldi, 9. Mare Australe, 10. Campbell, 11. Birkhoff, 12. Lorentz, 13. Mendeleev, 14. Korolev, 15. Schrodinger, 16. Hertzsprung, 17. Aitken, 18. Mare Ingenii, 19. Oppenheimer, 20. Poincaré.

TABLE II

List of Lunar Domes

Location – IV H108 (988, 19 L) indicates that the feature is located on Lunar Orbiter 4 high resolution photograph 108, framelet 988, 19 cm from the left margin of the photograph.

R – Reliability of dome identification on A to E scale.

	Location	Description	R
	Orbiter 2		
M33	(946, 19.5L)	Hills on crater floor	C
	(941, 19.5L)	Botryoidal fill	B
M75	(446, 7.2L)	Double ring	B
	(439, 8.4L)	Hills on crater floor	D
	(443, 18.6L)	Double ring	D
	Orbiter 3		
M120	(762, 13L)	Two cratered cones with summit pits	C
M121	(900, 21L)	Cratered cones and botryoidal fill	B
	(724, 11.9)	Cratered cones on floor of Tsiolkovsky	C
	(711, 17.4L)	Cratered cones on floor of Tsiolkovsky	C
	(692, 5.5L)	Dome in crater with sinuous rille	A
	(658, 20L)	Cratered cones	A
H199		Flamsted Ring	A
	Orbiter 4		
H5	(20, 5L)	Dome on mare ridge	A
H6	(180, 16.3L)	Dome on crater wall	B
	(182, 9L)	Cratered cone	C
	(201, 19L)	Domes on crater floor	C
	(227, 10.5R)	Isolated flat-topped domes	C
H8	(483, 9R)	Domes on crater floor	C
H9	(578, 12.7R)	Flat dome within irregular crater	A
H10	(672, 5L)	Domes on mare ridge	C
	(696, 14L)	Cratered cone within crater	C
H17	(623, 5.5L)	Textured dome in crater	D
H18	(755, 3L)	Cratered cones	D
H27	(983, 5L)	Hill on rille	C
	(983, 9.5L)	Hill at intersection of three rilles	C
H38	(415, 20L)	Dome on mare ridge	B
H52	(216, 11.5L)	Cratered flat-topped dome in crater	C
	(262, 21.5L)	Domes in three craters	A
	(265, 17L)	Rounded ridge in crater	D
H53	(373, 19.5L)	Aligned domes in crater	B
	(385, 16.5L)	Domes in crater	C
H60	(283, 9L)	Dome in crater	C
	(285, 23L)	Dome on mare ridge	B
	(277, 17L)	Double crater	A
H65	(935, 7L)	Dome associated with rille in crater	C
H66	(040, 10R)	Hummocky mass on crater floor	D
	(157, 19L)	Dome in the Palus Somnii	D
H67	(148, 17L)	Elongated domes in crater	C
	(169, 6L)	Double crater with domes in moat	A
	(255, 10R)	Flat-topped dome in crater	C
	(214, 18L)	Cratered dome	B

Table II (Continued)

	Location	Description	R
H68	(322, 16R)	Cratered cone on crater wall	A
	(368, 13.5R)	Double crater	A
	(368, 4.8L)	Broad dome on ridge	A
H70	(548, 4.5L)	Dome in crater	C
H71	(714, 9L)	Domes in Fabricus associated with rille	B
H72	(813, 10L)	Cratered domes associated with rille	B
	(815, 19L)	Domes in crater	B
	(818, 3.4)	Dome at crater intersection	A
	(819, 13.5L)	Large dome on crater floor	A
	(887, 15.5L)	Cratered cone	D
	(889, 5.7L)	Cratered cone	C
	(816, 15L)	Cratered cone associated with rille	C
	(816, 2R)	Dome field	D
	(838, 4.5L)	Dome in double crater	C
	(839, 16.5L)	Six domes on mare ridge	A
	(855, 10L)	Dome on crater rim	A
H74	(072, 20.5L)	Three peaks in crater	D
H76	(378, 2.5L)	Oversized central peak	D
H77	(526, 8R)	Irregular domes associated with rille	D
H78	(637, 19L)	Dome on mare ridge	A
	(593, 10L)	Pear shaped dome on mare ridge	C
	(611, 16R)	Cratered hill on crater wall	A
	(643, 7L)	Domes on mare ridge	B
H83	(259, 15L)	Swelling on ridge in crater	D
H84	(411, 7.5R)	Domes on floor of Theophilus	C
	(432, 8L)	Domes on crater rim	D
	(397, 18.7)	Cratered ellipsoidal hill	A
H86	(641, 14L)	Dome field	E
	(699, 3L)	Aligned hills	E
	(678, 8.5R)	Small domes	D
	(681, 13.5L)	Dome at crater intersection	D
	(682, 19.7L)	Cratered hill	D
	(683, 1.52L)	Cratered cone on crater wall	D
	(699–685)	Lacus Somniorum Dome Field	C-A
H88	(924, 9L)	Cratered hills in crater	D
	(904, 15.5R)	Cratered hill on crater wall	C
H89	(0.35, 9.5L)	Pear-shaped hill with summit crater	C
	(046, 14L)	Domes in crater	D
	(0.39, 7.5L)	Cratered cone	D
	(0.53, 4.5L)	Cratered hills on crater wall	C
	(059, 10.5L)	Three aligned hills	D
	(063, 2L)	Hills on crater wall	D
	(099, 9R)	Dome at crater intersection	C
	(074, 5L)	Domes on crater floor	C
H90	(200, 12R)	Domes associated with rille	C
	(215, 14L)	Domes in crater	D
H91	(324, 10L)	Dome Field, Lacus Mortis	B
	(336, 7L)	Dome Field, Lacus Mortis	C
	(357, 2L)	Dome associated with ridge	B
	(357, 6L)	Cratered dome in crater	A
	(349, 5.5L)	Cratered cone	A
	(345, 2L)	Dome associated with ridge	C

Table II (Continued)

	Location	Description	R
	(318, 19L)	Cratered cone in crater	C
	(343, 2.5L)	Cratered cone	B
	(322, 14.2L	Cratered cone	B
	(324, 14.7L)	Cratered cone	C
	(329, 5.2L)	Pear shaped cratered hill	C
	(338, 8.5L)	Cratered cone	D
	(349, 7L)	Cratered cone	C
	(321, 2L)	Cratered cone	B
	(364, 5.5L)	Cluster of irregular hills	E
H94	(717, 9.5L)	Off-center central peak	C
H95	(840, 0.5L)	Dome on crater wall	C
	(838, 0.5L)	Dome on crater wall	C
	(859, 4L)	Dome in crater with fracture	B
H96	(010, 3L)	Flat topped hills	E
	(014, 2L)	Cratered hill on crater wall	C
	(0.28, 12R)	Double crater	B
	(940, 12L)	Cratered cones	B
	(958–956)	Dome Field	C
	(993, 6L)	Domes in crater, dome cratered	B
H97	(99–104)	Dome Field	C
	(127, 4L)	Mare dome, cratered	D
	(128, 10.5L)	Cratered cone	D
	(155, 18L)	Domes in craters	C
	(168, 5L)	Four domes in crater	D
H98	(23,	Botryoidal fill	
	(266, 9L)	Dome in crater	B
	(270,	Dome in crater	
H101	(621, 13L)	Double crater	B
	(623, 5.5L)	Flat topped dome with summit sag	B
	(671, 17L)	Cratered central peak	C
H102	(762, 18L)	Dome field	C
	(788, 6R)	Swelling on mare ridge	B
	(810, 6L)	Domes in crater	C
H103	(888, 13L)	Low hills	E
	(909, 13L)	Cratered hills	C
	(928, 11L)	Cones to southeast of Cassini	D
	(953, 1L)	Three domes	D
H108	(577, 10L)	Oversized central peak	D
	(583, 12.5L)	Dome on wall of Arzachel	C
H109	(676)	Dome field	C
	(683, 19R)	Cratered dome	D
	(716)	Dome field	C
	(713, 14.5L)	Cratered cone	C
	(737, 12L)	Double crater	A
H110	(807, 7L)	Cratered cone	E
	(867, 3L)	Dome associated with rille	D
	(821, 2L)	Cratered cone	C
	(808, 1.5L)	Flat topped dome on crater wall	C
H112	(091, 16R)	Dome associated with rille	C
	(092, 11R)	Domes on crater floor	C
	(063, 19L)	Cratered central peak	C
H113	(188, 1L)	Dome associated with rille	A

Table II (Continued)

	Location	Description	R
	(188–193)	Five elongated domes	D
	(225, 14L)	Cratered cone	A
	(238, 11L)	Dome on mare ridge	B
	(240, 10.5L)	Swelling on mare ridge	A
	(263, 15L)	Flat topped irregular dome	C
	(269, 1L)	Three domes on crater floor	C
H114	(317, 10R)	Hemispheric dome	D
	(317, 7.5R)	Cratered cone	C
	(341, 16L)	Oversized central peak	C
	(340, 10L)	Cratered dome	D
	(350, 1.5L)	Cratered hill associated with ridge	D
	(354, 14L)	Domes in Eratosthenes	D
	(362, 10.5L)	Domes associated with ridge	D
	(366, 5L)	Oversized central peak	E
	(376, 1.5L)	Flat topped dome	D
	(405, 13R)	Irregular hill with summit sag	B
H115	(464, 8.2L)	Cratered cone	B
	(470, 22.5L)	Double crater	B
	(520, 17.5L)	Domes on mare ridge	D
	(507, 18.5R)	Cratered cone	C
	(510, 19.5R)	Dome associated with ridge	B
	(472, 6R)	Cratered cone	D
	(471, 21L)	Cratered cone	C
	(468, 16R)	Cratered cone	B
	(471, 5R)	Cratered cone	B
	(461, 6.5L)	Cratered cone	B
	(443, 8.5R)	Hummocky terrain	E
H116	(639, 12L)	Dome associated with ridge	D
	(641, 19R)	Cratered cone	C
	(604, 12L)	Dome cluster	C
H119	(010, 7L)	Domes on floor of Tycho	B
H120	(159, 17.5L)	Swelling on mare ridge	C
	(101–108)	Dome field in Fra Mauro Fm.	C
	(111, 15.5L)	Cratered cone	A
	(107, 1.5L)	Four cratered domes	C
H121	(304, 14L)	Cratered cone	B
	(209, 2L)	Domes on floor of Copernicus	B
	(299, 9R)	Elongated domes	C
	(307–318)	Dome field	C
H122	(402, 19.5L)	Dome on mare ridge	D
H124	(636, 4.5R)	Cratered dome in double crater	B
	(640, 17L)	Domes on crater floor	C
	(647, 4.5R)	Dome associated with rille	B
	(649, 7L)	Cratered hills and noncratered hills	B
	(654, 4.5L)	Cratered cone	B
H125	(836, 3.2L)	Cratered cone	C
	(773, 16R)	Dome on mare ridge	B
	(786, 5.5R)	Cratered ridge on mare ridge	B
	(798, 3L)	Dome with summit rift	B
H126	(941, 1.6L)	Cratered cone	C
	(942, 0.6L)	Two cratered cones	B
	(941, 1.8L)	Cratered cone	B

Table II (Continued)

	Location	Description	R
	(933, 11.5L)	Cratered cone	B
	(940, 4L)	Cratered cone	C
	(942, 0.5L)	Cratered cone	B
	(944, 9L)	Irregular dome	B
H127	(044, 10L)	Dome associated with mare ridge	D
	(017, 11R)	Swelling on mare ridge	C
H130	(440, 7.8L)	Cratered cone on crater rim	D
	(441, 5.5L)	Cratered cone	C
	(445, 8.4R)	Chain of domes in Moretus	B
	(433, 7R)	Irregular domes	B
H131	(542, 4.3L)	Cratered cone	C
H132	(686, 27L)	Small hemispheric hill with depression	C
	(693, 17.8L)	Swelling at mare ridge intersection	A
	(741, 13.5L)	Cratered cone at rille-crater intersection	B
H133	(863, 13L)	Mare dome, Milichius Dome	A
	(863, 10L)	Flat topped domes	B
	(838, 19.5L)	Six irregular hills	B
	(868–871)	Hortensius Domes	A
	(865, 14L)	Dome on mare ridge	B
	(879–888)	Hummocky Terrain	D
	(862, 9L)	Mare dome	A
H133	(860, 5L	Mare dome	A
	(854, 13L)	Mare dome	A
	(871, 1.7L)	Cratered cone	D
H134	(968, 6.8L)	Dome on mare ridge	B
	(224, 14L)	Dome-in-crater morphology	B
H137	(383, 2L)	Domes in Gassendi	B
	(353, 11.2R)	Dome on mare ridge	B
	(353, 7R)	Hill on mare ridge	B
	(353, 15.5R)	Irregular dome	C
H138	(544, 13.5L)	Dome on mare ridge	A
	(513, 7L)	Three domes	D
	(528, 18L)	Hummocky Terrain	D
H139	(598, 2R)	Oversized central peak	D
H142	(989, 11L)	Ridge associated with rille	A
	(985, 13L)	Dome associated with ridge	B
	(995, 8L)	Mare dome associated with rille	B
	(008, 4L)	Flat topped dome	B
	(012, 5L)	Cratered hill, textured	B
	(992, 9L)	Four aligned hills	B
H143	(134, 17.5L)	Four elongated domes	A
	(125–128)	Crater rim	B
	(139, 9.4L)	Mesa on mare ridge	A
	(140, 10L)	Flat topped hills forming circular pattern	A
	(255	Harbinger Mountains	C
H145	(488, 1L)	Domes in moat of double crater	A
	(444, 7L)	Gruthuisen domes	A
	(443, 24.5L)	Domes on mare ridge	C
	(445, 12.7L)	Domes on mare ridge	C
	(387, 7L)	Flat topped domes	D
H148	(784	Domes in crater	
	(773	Textured dome	

Table II (Continued)

	Location	Description	R
H149	(966, 15L)	Dome in Mersenius	C
	(992, 10.5L)	Flat topped domes in crater	C
H150	(044	Aristarchus Plateau	A
	(077	Marius Hills	A
H151	(164, 8.5L)	Double crater	C
	(165, 7L)	Elongated hill	D
	(166, 19L)	Flat topped hill	D
	(230, 21L)	Domes associated with rille	A
	(232, 13.2L)	Cratered cone	B
	(224, 4L)	Mare dome	B
	(164, 7.6L)	Double crater	A
	(164, 16L)	Double crater	B
	(165, 9.5L)	Dome in crater	B
H154	(598, 12.3L)	Crater with summit sag	D
H155	(697, 6.5K)	Flat topped hill	C
	(758, 19.8R)	Elongated dome	B
	(692, 0.7R)	Dome in rille	C
H156	(836, 5L)	Botryoidal fill	C
	(837, 15L)	Swelling on mare ridge	B
	(860, 15R)	Swelling on mare ridge	C
	(862, 12R)	Irregular hill	B
	(872, 13L)	Dome associated with ridge	B
	(891, 11R)	Cratered cone	C
H157	(999, 8.2R)	Cratered cone	A
	(998, 5.3R)	Cratered cone	A
	(999, 4L)	Cratered cone	A
H158	(090, 3L)	Three hills associated with ridge	D
	(100, 4.5L)	Irregular hill	D
	(131, 17L)	Mairan T, Cratered cone	B
	(156, 7L)	Elongated cones	A
	(127, 9.5L)	Textured dome	A
H160	(419, 11L)	Two cratered cones	D
	(363, 12L)	Irregular Hills	E
	(363, 15.5R	Cratered hills	C
	(356, 13.5R)	Irregular hills	E
	(406, 21L)	Flat-topped hill	D
H161	(504, 13.4L)	Flat-topped cratered hill	D
	(541, 6L)	Dome on floor of rille	C
	(497, 17L)	Domes on crater wall	C
	(497, 9L)	Dome on crater wall	B
	(488, 10L)	Hills on crater rim	C
	(485,	Hummocky terrain	C
H162	(690, 7L)	Cratered cone	B
	(679, 6L)	Domes in Cavalerius	B
	(667, 7R)	Mare dome	B
	(660, 7.5R)	Mare dome	C
	(663, 0.5R)	Mare dome	B
H163	(760, 15.4L)	Cratered hill	E
	(763, 4.8L)	Swelling at crater intersection	C
	(768, 19.5L)	Botryoidal fill	B
	(789,	Rümker Hills	A
	(808, 15.5L)	Mare dome	B

Table II (Continued)

	Location	Description	R
	(798, 19.5L)	Mare dome	B
H165	(072, 6L)	Six cratered cones	B
	(066, 11L)	Textured domes in crater	C
	(067, 3L)	Hummocky terrain	D
	(010, 13.5L)	Flat-topped dome	C
	(011, 17L)	Flat-topped domes	C
H166	(148, 8.5L)	Cratered dome	D
	(148, 13L)	Cratered cone on crater rim	C
H167	(279, 10.5L)	Domes within crater	D
	(299, 8L)	Flat-topped domes in crater	C
H168	(426, 10.5L)	Aligned hills	D
	(423, 6L)	Dome on crater floor	D
	(409, 8R)	Flat-topped hill	D
	(406, 16.5R)	Domes in crater	D
H169	(595, 12.5L)	Cratered cone associated with rille	B
	(584, 13.5R)	Domes in crater	D
	(573, 5L)	Domes floor of Kraft	C
H174	(237, 15.7R)	Large cratered cone	B
	(205, 13.5L)	Dome on crater wall	C
H175	(379, 16L)	Mare dome	B
	(378, 20L)	Aligned hills	C
H176	(505, 10L)	Domes in Pythagoras	B
	(506, 14L)	Dome in Pythagoras	B
	(491, 11L)	Dome in crater	B
H177	(624, 19.5L)	Flat dome	C
	(740 13L)	Large dome in crater	C
H178	(762, 15L)	Dome at intersection of rille and crater	B
H179	(899, 8L)	Cratered hill	D
	(890, 7.5L)	Hill at crater intersection	E
	(888, 10L)	Dome on crater wall	C
H181	(118, 19L)	Cratered domes	C
	(154, 4L)	Flat-topped domes	A
	(167, 7.5)	Dome in crater	B
H182	(238, 9.5R)	Five aligned domes	B
	(267, 7L)	Domes in crater	C
	(265, 17L)	Domes in crater	C
	(285, 3.5L)	Hill at rille intersection	D
	(282, 5L)	Cratered cone on ridge	B
	(305, 14.5L)	Domes in crater	B
H183	(423, 0.5L)	Dome in crater	D
	(422, 1.3L)	Cratered cone	B
	(416, 6.5L)	Double crater	C
	(385, 11L)	Domes in crater	D
	(409, 7L)	Cratered dome	B
	(420, 1.5L)	Textured dome	A
	(433, 13L)	Botryoidal fill	B
	(446, 14.5L)	Aligned domes in crater	C
H184	(549, 5R)	Central peak Petavius	C
H186	(759, 5R)	Domes in crater	B
	(770, 22L)	Domes in crater	B
	(806, 15L)	Domes in crater	B
	(838, 16L)	Domes on mare ridge	C

Table II (Continued)

	Location	Description	R
H187	(928, 22L)	Domes in crater	D
	(938, 7L)	Mare dome	C
	(938, 8L)	Mare dome	C
	(943, 5L)	Mare dome	C
	(951, 9L)	Cratered domes	B
H188	(051, 17L)	Domes in Einstein	B
H189	(203, 21.5L)	Double crater	B
	(211, 24L)	Textured hill	D
	(154, 14.5L)	Botryoidal fill	C
H191	(456, 10.5L	Flat-dome in crater	C
	(460, 4.5L)	Flat-topped dome in crater	C
H192	(555, 9.5L)	Cratered cone	C
	(556, 11L)	Cratered cone	C
	(572, 15L)	Dome in crater	C
	(579, 17L)	Domes in Geminus	C
H193	(718, 12L)	Domes in crater	C
H195	(978, 15L)	Domes in crater	C
	(999, 14L)	Dome and flow, Mare Orientale	A
	(002, 13L)	Layered mare dome	A
	Orbiter V		
H6	(295, 14L)	Dome at crater intersection	D
H18	(869, 14R)	Dome in crater	D
H20	(122, 8.4L)	Cratered cone	C
M40		Domes on floor of Stevinus	C
M43	(304, 10.5L)	Domes in crater	E
M65	(189, 11.5L)	Domes on mare ridge	B
	(180, 13L)	Dome in crater	B
	(187, 11L)	Dome in crater	C
H79	(811, 4.3L)	Cratered cone	C
H103	(944, 21L)	Two double craters	C
H151	(252, 18L)	Cratered cone	B
	(250, 17L)	Hill associated with rille	C
M152		Domes on floor of Copernicus	A
M177	(901, 12L)	Domes on mare ridge	B
M179	(147, 8L)	Dome at rille intersection	C
	(154, 26L)	Dome in crater	C
M183	(451, 18L)	Three domes in crater	C
M201		Domes on floor of Kepler	A

origin of sinuous rilles is controversial; but their origin is probably related to an endogenic process (Greeley, 1970; Schumm, 1970) and dark halo craters have been interpreted as volcanic features (Kuiper *et al.*, 1966). The association and similar distribution of domes, sinuous rilles and dark halo craters suggests that they have a similar origin (all are related to endogenic processes).

(3) Domes are rarely found in the central portions of the circular basins (for example, Mare Imbrium and Humorum).

(4) Domes are in general concentrically arranged about circular basins. Few domes are related to radial sculpture. This suggests that concentric patterns may be related

to deep-seated fractures which are in places controlled by the lunar tectonic grid (see point 5). Radial sculpture, on the other hand seems to represent a surficial layer with no deep-seated connections. Hartmann and Wood (1971) reached a similar conclusion by observing that radial structure is obscured faster than concentric structure as a basin ages. This occurs because radial systems are primarily surficial, of low relief and easily blanketed by ejecta and regolith whereas concentric systems have greater relief and possibly deep-seated structural control, and as a result retain topographic relief longer (Hartmann and Wood, 1971).

(5) Domes are locally controlled by the lunar grid (Strom, 1964). Domes are on mare ridges and rilles elongated in a grid direction; in several places domes themselves are aligned in a grid direction and in places location may be controlled by grid intersections. Grid control around basins may be secondary, that is grid lineaments were present before the formation of the basins and were subsequently rejuvenated or activated by basin formation. With more data, concentric patterns about basins may resolve into grid directions. For example, concentric mare ridge patterns in Mare Imbrium can be resolved into segments controlled by the lunar grid (Elston *et al.*, 1971).

(6) Dome formation spans a wide range of lunar time. Presently observed domes are associated with old mare materials in Mare Smythii and Tsiolkovsky and are on the floors of young craters such as Tycho and Copernicus. Domes were probably not formed during one great lunar effusive event, but each dome-forming episode is probably related to the formation of individual craters and mare basins and to basin-filling episodes. Activity in areas where domes are located may be continuing to the present as seen by the close correlation between dome distribution and the distribution of lunar transient events. Middlehurst (1967) concluded that lunar transient events occur (a) near the border of the maria especially about Mare Imbrium, Serenitatis, Crisium and Humorum; (b) associated with ray craters (e.g., Tycho, Copernicus, Aristarchus and Kepler); (c) in ring craters with dark mare or partially dark floors (e.g., Plato, Grimaldi and Alphonsus). Transient lunar events have not been reported from the central parts of the circular basins. Transient events therefore occur in the same general areas as domes, rilles and dark halo craters. Middlehurst and Moore (1967) previously recognized the correlation of sites of lunar events with the distribution of dark halo craters. Moore (1971) added 313 additional events to Middlehurst's list of 400; however these additional data do not change the distribution. This correlation does not necessarily infer that domes, sinuous rilles and dark halo craters are presently active; however one may speculate that the areas where these features occur are the sites of recent activity; perhaps in the form of isolated gas discharges.

(7) Domes are not restricted to the equatorial areas of the Moon or maria as suggested by Arthur (1962) Baldwin (1963) Brungart (1964) and others. This illusion was due to the fact that on Earth-based photographs domes were more easily observed on the maria and the fact that more mare material is present near the equator than elsewhere on the Moon's Earth-side.

(8) Dome distribution does not correlate well with gravimetric and acceleration

data (Muller and Sjorgen, 1968), deviation from the best fitting ellipsoid (Runcorn and Shrubshall, 1968) or infrared thermal anomalies (Shorthill and Saari, 1966). Domes are on the margins of basins with gravity highs of 60 mgals. Other than this, no other agreement between dome distribution and gravimetric data is obvious. A poor correlation exists between dome distribution and deviation from a best fitting ellipsoid (Runcorn and Shrubshall, 1968). Domes are on highs (positive deviations from the ellipsoid) in Oceanus Procellarum, Sinus Medii and Mare Tranquillitatis; otherwise no obvious correlation is observed. The alignment of the Rümker Hills, Aristarchus Plateau and Marius Hills along the axis of the Oceanus Procellarum on a 0.5–1.5 km bulge has been suggested as evidence that the area overlies an up-welling convection cell (McCauley, 1967). The distribution of domes does not correspond to locations of infrared thermal anomalies other than the fact that fresh craters which contain domes may be hot spots and vice versa.

(9) Domes at times group into volcanic complexes; for example the Rümker Hills, Aristarchus Plateau and Marius Hills. In these complexes, domes are commonly associated with flows, rilles and dark halo craters.

6. Conclusions

This paper presents criteria for the identification of lunar domes based on modification, location and morphology and shows:

(1) Many terrestrial volcanic extrusive domes are similar in morphology to some lunar domes. This analogy suggests that extrusive volcanic domes are indeed present on the Moon.

(2) Over 400 domes are present on the lunar surface, and are interpreted as having formed by endogenic processes.

(3) Many domes and other endogenic features on Figure 17 are related to basins and craters, and not to any observable moonwide pattern. Local control by the tectonic grid is, however, an exception. Domes are not uniquely found on maria.

(4) Activity in areas where domes are located may be continuing in the form of gas emissions to the present as revealed by the correlation of dome distribution with reported transient lunar events.

(5) The rock type and chemistry of domes is difficult to ascertain from study of Orbiter photographs. Earlier workers (McCauley, 1967, for example) assumed that low mare-type domes were basaltic and that lunar domes with steeper slopes and textured surfaces were formed by intermediate and felsic rocks. Even though this relationship may be true in some instances, a general rule can not be applied. For example, on Earth both basalts and rhyolites form broad shields and both form cone-shaped extrusions with slope angles on the flanks between 30–35° (Smith, 1970). Many domes are composed entirely of debris or mantled by rubble which stands at or near the angle of repose and controls the outward appearance of the dome. In these, morphology is essentially independent of composition. Too many variables exist therefore to make suggestions about dome rock type based on photogeologic studies alone.

Acknowledgments

This paper reports on a portion of a study which compares volcanic domes in the Mono Craters in California, and a dome complex in southwestern New Mexico with lunar volcanic features. I thank Wolfgang E. Elston of the University of New Mexico for reviewing the manuscript and offering many helpful suggestions. Research was supported by NASA grant NGL-32-004-011.

References

Abbey, L. B. and Both, E. E.: 1958, *Strolling Astron.* **12**, 96.
Alter, D.: 1957, *Publ. Astron. Soc. Pacific* **69**, 245.
Arthur, D. W. G.: 1962, *Commun. Lunar Planet. Lab.* **1**.
Baldwin, R. B.: 1963, *The Measure of the Moon*, University of Chicago Press, 488 pp.
Beswick, J. D.: 1962, *British Astron. Assoc. J.* **72**, 119.
Brungart, D. L.: 1964, 'The Origin of Lunar Domes', Thesis, Air Force Institute of Technology, MECH/GSF-64-32, 191 pp.
Bülow, Kurt Von: 1964, *Geologie* **13**, 449.
Eggleton, R. E.: 1970, 'Recognition of Volcanoes and Structural Patterns in the Rümker and Montes Riphaeus Quadrangles of the Moon', Ph.D. dissertation, University of Arizona, Tucson, 266 pp.
El-Baz, Farouk: 1971, *Apollo 14, Preliminary Science Report,* NASA SP-272, 267–274.
El-Baz, Farouk and Wilshire, H. G.: 1969, *Apollo 8, Preliminary Science Report*, NASA SP-201, 32–33.
Elston, W. E.: 1967, *Am. Astron. Soc.* **14**, 213.
Elston, W. E., Laughlin, A. W., and Brower, J. A.: 1971, *J. Geophys. Res.* **76**, 5670.
Fielder, G.: 1962, *British Astron. Assoc. J.* **72**, 24.
Greeley, Ronald: *Science* **172**, 722.
Hartmann, W. K. and Wood, C. A.: 1971, *The Moon* **3**, 3.
Herring, A. K.: 1960, *Sky Telesc.* **20**, 219.
Jamieson, H. D. and Rae, W. L.: 1965, *Brit. Astron. Soc. J.* **75**, 310.
Kuiper, G. P., Strom, R. G., and Le Poole, R. S.: 1966, in *Ranger VIII and IX*, Part 11, NASA Technical Report No. 32-800, 35–248.
McCauley, J. F.: 1967, in S. K. Runcorn (ed.), *Mantles of the Earth and Terrestrial Planets*, Interscience, New York.
McCauley, J. F.: 1968, *Amer. Inst. Aeron. Astron. J.* **6**, 1991.
McCauley, J. F.: 1969, *Trans. Amer. Geophys. Union* **50**, 229.
Middlehurst, B. M.: 1967, *Rev. Geophys.* **5**, 173.
Middlehurst, B. M. and Moore, P.: 1967, *Science* **155**, 449.
Moore, P.: 1971, *British Astron. Assoc. J.* **81**, 365.
Moore, P. and Cattermole, P. J.: 1957, *J. Intern. Lunar Soc.* **1**, 16.
Muller, P. M. and Sjogren, W. L.: 1968, *Science* **161**, 680.
Murray, J. B. and Guest, J. E.: 1970, *Modern Geology* **1**, 149.
O'Keefe, J. A., Lowman, P. D., and Cameron, W. S.: 1967, *Science* **155**, 77.
Pickering, W. D.: 1903, *The Moon,* Doubleday, Page and Co., New York.
Putnam, W. C.: 1938, *Geograph. Rev.* **38**, 68.
Rae, W. L.: 1963, *Brit. Astron. Assoc. J.* **73**, 165.
Rae, W. L.: 1966, *Brit. Astron. Assoc. J.* **76**, 319.
Runcorn, S. K. and Shrubshall, M. H.: 1968, *Phys. Earth Planetary Interiors* **1**, 317.
Schumm, S. A.: 1970, *Geol. Soc. Am. Bull.* **81**, 2539.
Scott, D. H., West, M. N., Lucchitta, B. K., and McCauley, J. F.: 1971, *Apollo 14, Preliminary Science Report,* NASA SP–272, 274–283.
Shaler, N. S.: 1903, *Smithsonian Contrib. Knowledge* **34**, 1.
Shorthill, R. W. and Saari, J. M.: 1966, in W. N. Hess, D. H. Menzel, and J. A. O'Keefe (eds.), 'The Nature of the Lunar Surface', *Proceedings of the 1965 IAU-NASA Symposium*, Baltimore, p. 215.
Smith, E. I.: 1969, *Trans. Amer. Geophys. Union* **50**, 229.

Smith, E. I.: 1970, 'A Comparison of Selected Lunar and Terrestrial Volcanic Domes', Ph.D. dissertation, University of New Mexico, Albuquerque, 200 pp.
Smith, E. I.: 1971, *J. Geophys. Res.* **76**, 5683.
Spurr, J. E.: 1944, *Geology Applied to Selenology*, Vol. 1, Science Press Printing Co., Lancaster, Pa., 112 pp.
Strom, R. G.: 1964, *Commun. Lunar Planet. Lab.* **205**, 39.
Strom, R. G.: 1971, *Modern Geology* **2**, 133.
Westfall, J. E.: 1964, *Strolling Astron.* **18**, 15.
Williams, H.: 1932a, *Univ. Calif. Pub., Bull. Dept. Geol. Sci.* **21**, 51.
Williams, H.: 1932b, *Univ. Calif. Pub., Bull. Dept. Geol. Sci.* **21**, 195.